

<https://doi.org/10.1038/s42003-024-06706-4>

Nasal symbiont *Staphylococcus epidermidis* restricts influenza A virus replication via the creation of a polyamine-deficient cellular environment

Check for updates

Ara Jo^{1,8}, Kyeong-Seog Kim^{1,2,3,8}, Jina Won¹, Haeun Shin¹, Sujin Kim¹, Bora Kim^{2,6}, Da Jung Kim^{2,7}, Joo-Youn Cho^{1,2,3,8} & Hyun Jik Kim^{1,2,4,5,8}

Studies on the immune-regulatory roles played by the commensal microbes residing in the nasal mucosa consider the contribution of antiviral immune responses. Here, we sought to identify the nasal microbiome, *Staphylococcus epidermidis*-regulated antiviral immune responses and the alteration of polyamine metabolites in nasal epithelium. We found that polyamines were required for the life cycle of influenza A virus (IAV) and depletion of polyamines disturbed IAV replication in normal human nasal epithelial (NHNE) cells. Inoculation of *S. epidermidis* also suppressed IAV infection and the concentration of polyamines including putrescine, spermidine, and spermine was completely attenuated in *S. epidermidis*-inoculated NHNE cells. *S. epidermidis* activated the enzyme involved in the production of ornithine from arginine and downregulated the activity of the enzyme involved in the production of putrescine from ornithine in nasal epithelium. *S. epidermidis* also induced the activation of enzymes that promote the extracellular export of spermine and spermidine in NHNE cells. Our findings demonstrate that *S. epidermidis* is shown to be able of creating an intracellular environment lacking polyamines in the nasal epithelium and promote the balance of cellular polyamines in favor of the host to restrict influenza virus replication.

It is becoming increasingly apparent that the primary targets of respiratory viruses, including influenza viruses, are the respiratory epithelium, and that the innate immune system of the respiratory epithelium serves as the first line of defense in the suppression of respiratory virus infection^{1,2}. The respiratory epithelium produces antiviral molecules that initiate immune responses by rapid recruitment of innate effector cells and have their own unique mechanisms to prime antiviral immune responses in the respiratory tract against influenza viruses^{3–5}. Importantly, the colonizing microbiome in the human respiratory mucus is subject to mediate the mucosal immune defense mechanisms of the respiratory epithelium, and studies on the reaction of the mucosal microbiome to the inhaled pathogens within the host increasingly consider the contribution of immune responses^{6,7}. Inhaled

respiratory viruses encounter the host's immune system for the first time in the nasal passage, and the microbial characteristics of the nasal mucus are closely related to the mechanisms of initial immune responses^{8,9}. Thus, insights into the microbiota of the human nasal mucus can provide fundamental information about the susceptibility of an individual to respiratory viral infections and factors contributing to related immune mechanisms^{10,11}. Our previous study revealed that *Staphylococcus epidermidis* was the most abundant commensal present in the nasal mucus of healthy humans and that it accelerated the clearance of influenza A virus (IAV) from the nasal epithelium⁸. In addition, the inoculation of the human nasal commensal *S. epidermidis* into an *in vivo* nose limited IAV-caused lung infection via interferon-related innate immune responses¹².

¹Department of Otorhinolaryngology, Seoul National University College of Medicine, Seoul, Republic of Korea. ²Department of Clinical Pharmacology and Therapeutics, Seoul National University College of Medicine and Hospital, Seoul, Republic of Korea. ³Department of Biomedical Sciences, Seoul National University College of Medicine, Seoul, Republic of Korea. ⁴Seoul National University Hospital, Seoul, Republic of Korea. ⁵Sensory Organ Research Institute, Seoul National University Medical Research Center, Seoul, Republic of Korea. ⁶Present address: Center for Cancer Research, National Cancer Institute, National Institutes of Health, Bethesda, MD, USA ⁷Present address: Liver Research Institute, Seoul National University College of Medicine, Seoul, Republic of Korea ⁸These authors contributed equally: Ara Jo, Kyeong-Seog Kim, Joo-Youn Cho, Hyun Jik Kim. e-mail: joocho@snu.ac.kr; hyunjerry@snu.ac.kr

A virus has to infect host cells to complete the genome replication and transcription, and the reproduction of a new infectious virus through its own metabolic machinery and enzyme system¹³. In this process, polyamines including putrescine, spermidine, and spermine are small aliphatic metabolites synthesized by mammalian cells to support cellular processes such as cell cycling and viruses rely on polyamines for the varied stages of replication, including cell binding, viral transcription and protein translation^{14,15}. In the metabolic pathway of biogenic polyamines, ornithine is converted to putrescine by ornithine decarboxylase 1 (ODC1), and it follows that putrescine is converted to spermidine by spermidine synthetase (SRM) and spermine by spermine synthetase (SMS)¹⁵. Several specific and potent inhibitors of the polyamine biosynthetic pathway have been developed to suppress viral replication and the ODC1 inhibitor, difluoromethylornithine (DFMO) which is approved by the Food and Drug Association, has been found to reduce the replication of diverse viruses in vitro and in vivo with minimal cytotoxicity¹⁶. Prior work has demonstrated that RNA viruses are sensitive to polyamine inhibitors in vitro, suggesting that polyamines might be necessary for the replication of respiratory viruses^{17,18}.

Complex host–microbe interactions have made it difficult to gain a detailed understanding of the mechanisms involved in the cellular metabolism and antiviral immune responses. However, we hypothesized that nasal commensals that are always present in the nasal mucus or microbe-secreted proteins could affect the metabolites of the nasal mucosa. In particular, if the concentration of polyamines can be altered by the symbiotic nasal microbiome, respiratory virus replication could be controlled at the level of nasal epithelium and viral spread to the lower airway might be restricted more efficiently.

In this study, we aimed to determine whether *S. epidermidis*, a dominant nasal commensal in healthy nasal mucus, might have the ability to influence the environment of cellular metabolites in the nasal mucosa and whether the alteration of metabolites might be involved in the suppression of IAV replication. We show that *S. epidermidis* creates an intracellular environment lacking polyamines in the nasal epithelium to restrict IAV

replication and promote the balance of cellular polyamines in favor of the host.

Results

Nasal commensal *S. epidermidis* alters the metabolites in nasal epithelium

We first sought to explore whether the metabolite profile might be altered in nasal epithelium via human nasal commensal *S. epidermidis*. NHNE cells from five healthy volunteers (Supplementary Table S1) were inoculated with *S. epidermidis* (multiplicity of infection (MOI) = 0.25) for 1 day and the metabolome analysis was performed in the NHNE cell lysates using a p180 kit for screening of differential metabolomic profiles.

We compared NHNE cell lysates of 111 metabolites depending on *S. epidermidis* inoculation by partial least squares-discriminant analysis (PLS-DA), and separated profiles were observed (Fig. 1A). A variable importance in projection score plot followed by PLS-DA analysis is shown in Fig. 1B. The most important metabolites upregulated in *S. epidermidis*-inoculated NHNE cells were citrulline, ornithine, acetylornithine, glutamate, and aspartate. To determine the specific metabolism altered in NHNE cells after inoculation with *S. epidermidis*, we used a metabolite set enrichment analysis (MSEA) approach using the small molecule pathway database (SMPDB) (Fig. 1C) and visualized the biochemical and chemical interactions of metabolites (Fig. 1D, E). Together, the urea cycle and polyamine-related metabolites were altered significantly. The urea cycle-related metabolites such as citrulline (fold change 154.1), ornithine (fold change 32.47), and acetylornithine (fold change 29.25) were upregulated, whereas arginine was decreased (fold change -4.69). Polyamines (putrescine, spermidine, and spermine) were downregulated with a fold change of -3.33 to -1.66. Additionally, other metabolisms were also altered, for instance, arginine and proline metabolism, glycine and serine metabolism, and phosphatidylethanolamine (PE) biosynthesis (Fig. 1C). In lipid metabolism, the levels of most lipids were decreased including phosphatidylcholines (PC), PEs, and sphingomyelins (SM) (Fig. 1E).

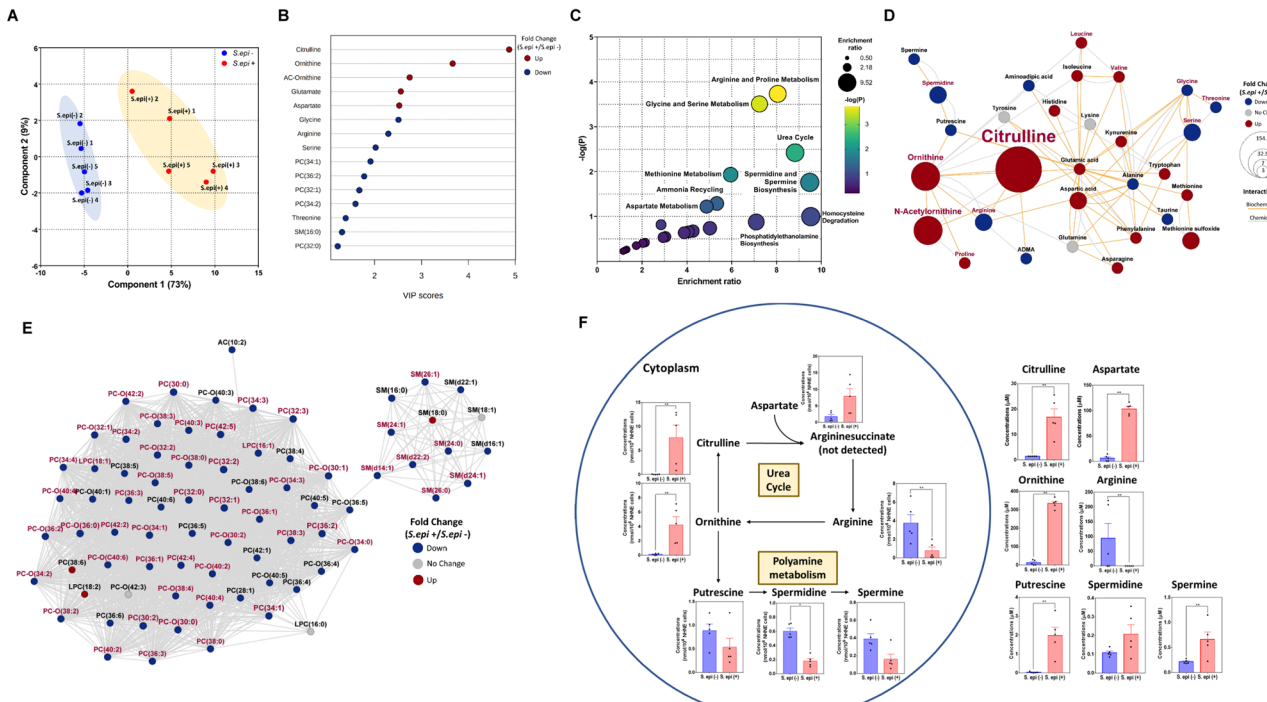


Fig. 1 | Nasal symbiont *S. epidermidis* alters the concentration of metabolites and metabolic pathways. **A** PLS-DA score plot, **B** VIP score plot showing top 15 metabolites by component 1, **C** metabolites set enrichment analysis using SMPDB,

and chemical and biochemical networks of **(D)** amino acids and biogenic amines and **(E)** lipids. **F** Mapping of the urea cycle and polyamine metabolism-related metabolites from *S. epidermidis*-inoculated NHNE cells.

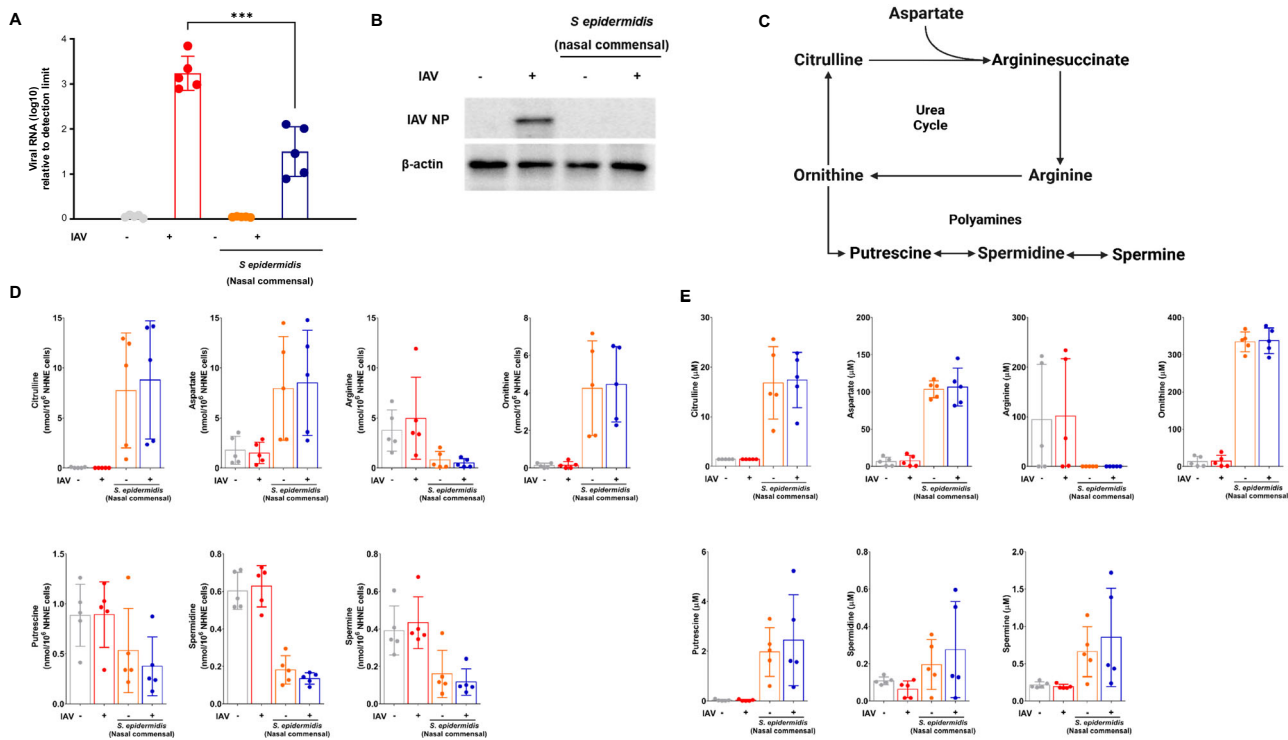


Fig. 2 | *Staphylococcus epidermidis* restricts IAV replication through the induction of polyamine depletion in nasal epithelial cells. *Staphylococcus epidermidis* restricts IAV replication through the induction of polyamine depletion in nasal epithelial cells. A Schematic diagram of the urea cycle and polyamine

metabolism, B IAV PA mRNA expression, C NP protein expression, and changes in the urea cycle and polyamine metabolism-related metabolites in (D) cell lysate and (E) supernatant.

As the urea cycle and polyamine-related metabolites were changed significantly in NHNE cells after the inoculation of *S. epidermidis*, we mapped those metabolisms with detected metabolites from cell lysate and the supernatant (Fig. 1F). Interestingly, urea cycle-related metabolites were changed in the same direction in both lysate and supernatants. However, the concentrations of polyamines were downregulated in cell lysate but upregulated in the supernatant in response to *S. epidermidis* inoculation. These results indicate that the inoculation of the human nasal microbiome with *S. epidermidis* alters metabolic profiles and, in particular, depletes the polyamines from the intracellular level while the urea cycle metabolites are upregulated.

***Staphylococcus epidermidis* restricts IAV replication and mediates polyamine depletion in nasal epithelium**

To determine the effects of *S. epidermidis* pretreatment on the susceptibility of the nasal epithelium to IAV infection, NHNE cells were inoculated with *S. epidermidis* (MOI = 0.25) at 8 h before IAV infection (WS/33, H1N1 MOI = 1) and the concentration of polyamines and the transcription or translation levels of IAV were measured. The real-time PCR results revealed that the increase in IAV PA RNA level (1.5×10^3) was significantly attenuated in IAV-infected NHNE cells after inoculation of *S. epidermidis* (3.9×10^2) at 1 dpi (Fig. 2A). Similarly, *S. epidermidis* exposure also decreased IAV NP levels in the cell lysate of IAV-infected NHNE cells at 1 dpi (Fig. 2B).

Next, we compared the metabolite levels related to the urea cycle (citrulline, aspartate, arginine, citrulline, and ornithine) and polyamine metabolism (putrescine, spermidine, and spermine) from NHNE cell lysate and supernatant after the inoculation of *S. epidermidis* or IAV (Fig. 2C). The concentrations of urea cycle-related metabolites such as citrulline, aspartate, and ornithine were increased in the cell lysate in response to *S. epidermidis*, whereas arginine was decreased (Fig. 2D). A similar pattern of metabolite concentration changes was also observed in the supernatant of NHNE cells inoculated with *S. epidermidis* (Fig. 2E). While the level of ornithine was

highly elevated, the concentration of polyamines such as putrescine, spermidine, and spermine was significantly lower in the cell lysate of *S. epidermidis*-inoculated NHNE cells (Fig. 2D). Interestingly, the concentration of polyamines increased in the supernatant of NHNE cells after inoculation with *S. epidermidis* (Fig. 2E). In addition, metabolite profiles from NHNE cells after the inoculation of IAV did not separate by PLS-DA (Supplementary Fig. S1a) and the concentration of polyamine and urea cycle-related metabolites was not significantly altered in IAV-infected NHNE cells (Supplementary Fig. S1b). These findings suggest that human nasal commensal *S. epidermidis* restricted IAV replication in nasal epithelium and inoculation with *S. epidermidis* mediated the increase of urea cycle metabolites and depletion of polyamines in the nasal epithelium.

Polyamine depletion limits IAV replication in NHNE cells

As a next step, we examined whether polyamines might be essential for IAV replication in nasal epithelium and whether IAV replication was limited after the depletion of polyamines in NHNE cells. First, NHNE cells were treated with diethylnorspermidine (DENSpM, 100 μ M) and DFMO (100 μ M) which are known to mediate the depletion of polyamines at an intracellular level^{19,20}. We found that DENSpM treatment depleted the level of polyamines more significantly than DFMO in NHNE cells (Supplementary Fig. S2). Thus, to determine the influence of polyamine depletion on IAV replication, the NHNE cells were treated with DENSpM 8 h before IAV infection (MOI = 1) (Fig. 3A). The western blot results showed the increase in spermidine/spermine acetyltransferase 1 (SAT1) expression in NHNE cells after the addition of DENSpM and as expected, the polyamines were depleted in NHNE cells (Fig. 3B, C). We observed a significant reduction in viral RNA levels (Fig. 3D) and IAV NP expression (Fig. 3F) at 1 dpi in the cell lysate of IAV-infected NHNE cells following the addition of DENSpM. To determine if exogenously supplied synthetic polyamines serve to induce viral replication, NHNE cells were treated with synthetic polyamines (putrescine, spermine, and spermidine combined at 1 μ M) at 8 h before IAV infection. The results showed that both IAV PA RNA and NP

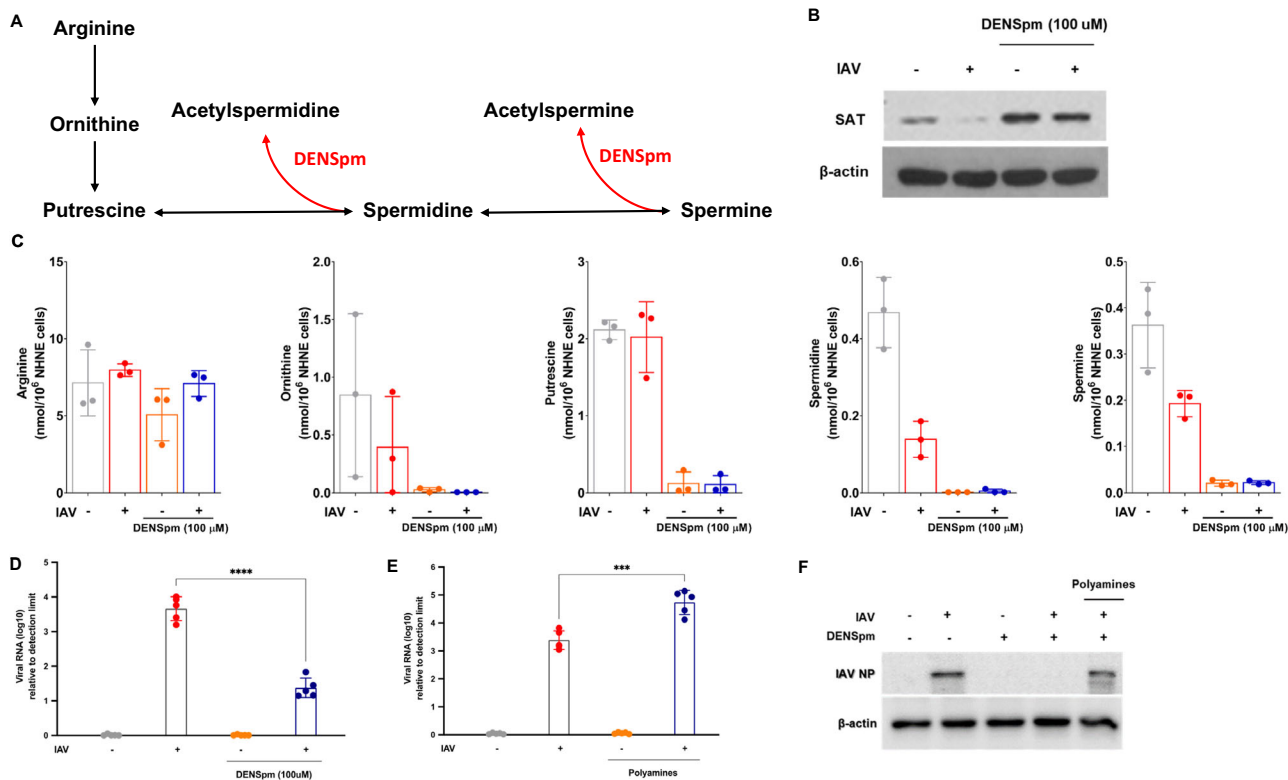


Fig. 3 | Polyamine depletion limits IAV replication in NHNE cells. **A** Schematic mechanism of the depletion of polyamines by DENSpm. **B** SAT1 protein expression. **C** Alterations of polyamine metabolism-related metabolites. **D, E** viral PA mRNA

expression by treating DENSpm or synthetic polyamines, and **F** viral NP protein expression. DENSpm-N1 N11-diethylnorspermine, SAT1 spermidine/spermine N1, acetyltransferase, PA polymerase, NA neuraminidase.

protein levels were significantly elevated in IAV-infected NHNE cells when the synthetic polyamines were added to the cells after DENSpm treatment (Fig. 3E, F). Together, these results suggest that polyamines are required for IAV replication in NHNE cells and the polyamine-depleted cellular environment limits the transcription and translation of IAV in nasal epithelium.

Staphylococcus epidermidis creates a polyamine-depleted cellular environment by affecting enzymes involved in polyamine production

Lastly, we sought to delineate precisely how *S. epidermidis* alters the concentration of polyamines in NHNE and shapes a polyamine-depleted cellular environment. The core polyamine synthesis pathway present in mammals is summarized in Fig. 4A. Within the cell, arginine is converted to ornithine, and arginase (ARG) is a critical enzyme in the biosynthesis of ornithine from arginine and ornithine. Ornithine is converted into the polyamine putrescine via the action of ODC1. Putrescine is converted into spermidine via the action of SRM; spermidine is converted into spermine via SMS. Spermine can be catabolized further back to spermidine and putrescine via the action of SAT1. We have already found that the concentration of ornithine was significantly higher and the concentration of putrescine, spermine, and spermidine was completely lower in the cell lysate of NHNE cells in response to *S. epidermidis*. Therefore, we presumed that *S. epidermidis* might affect enzymes that are involved in the production of polyamines in nasal epithelium. We measured the mRNA levels of ARG, ODC1, and SAT1 in NHNE cells after inoculation with *S. epidermidis*. The results showed that the transcription of ODC1 was completely reduced in the cell lysate of NHNE cells 8 h after the inoculation of *S. epidermidis*. On the contrary, the mRNA levels of ARG and SAT1 were significantly elevated in response to *S. epidermidis* from 1 dpi (Fig. 4B). The western blot results also showed that the expression of ODC1 gradually decreased 8 h after inoculation with *S. epidermidis* and the expression of both ARG and SAT1 was significantly induced in NHNE cells from 1 dpi (Fig. 4C). These results

suggest that *S. epidermidis* shifted an intracellular environment in the direction of reducing polyamine synthesis and induced the export of polyamines from the NHNE cells.

Discussion

Our study revealed that human nasal commensal *S. epidermidis* might shape a polyamine-depleted cellular environment by affecting the enzymes involved in urea cycle metabolism and polyamine production resulting in the disturbance of IAV replication in the nasal epithelium. Here, we found that polyamines are essential for IAV replication in nasal epithelium and are required for the transcription or translation of IAV. Following inoculation with *S. epidermidis*, the concentration of cellular polyamines, including putrescine, spermine, and spermidine, was altered in the nasal epithelium, thereby skewing the polyamine balance of the nasal mucosa in favor of the host. We estimate that the depletion of polyamines by *S. epidermidis* contributes to restrict IAV replication in nasal epithelium and these observations makes an advance in our understanding of the antiviral mechanism of nasal commensal, *S. epidermidis*.

The respiratory mucosa is the first target organ of environmental pathogens and the critical role of the respiratory mucosa as a barrier for restricting invasion of the host by respiratory viruses has been emphasized^{21,22}. The compositional differences in the respiratory microbiome have drawn increased interest, and the importance of the respiratory microbiome, especially in immune protection, has been recognized²³. There is also growing evidence that a microbiome community resides in the human nasal mucus and exhibits the potential for antiviral immunity regulated by nasal microbiome. Our previous study revealed that *S. epidermidis* is the most abundant commensal organism in the healthy human nasal mucus, and the presence of *S. epidermidis* strengthens the frontline antiviral immune defense response in the nasal mucosa through the modulation of innate immune mechanisms¹². The current study also demonstrated that the transcription and translation of IAV were significantly

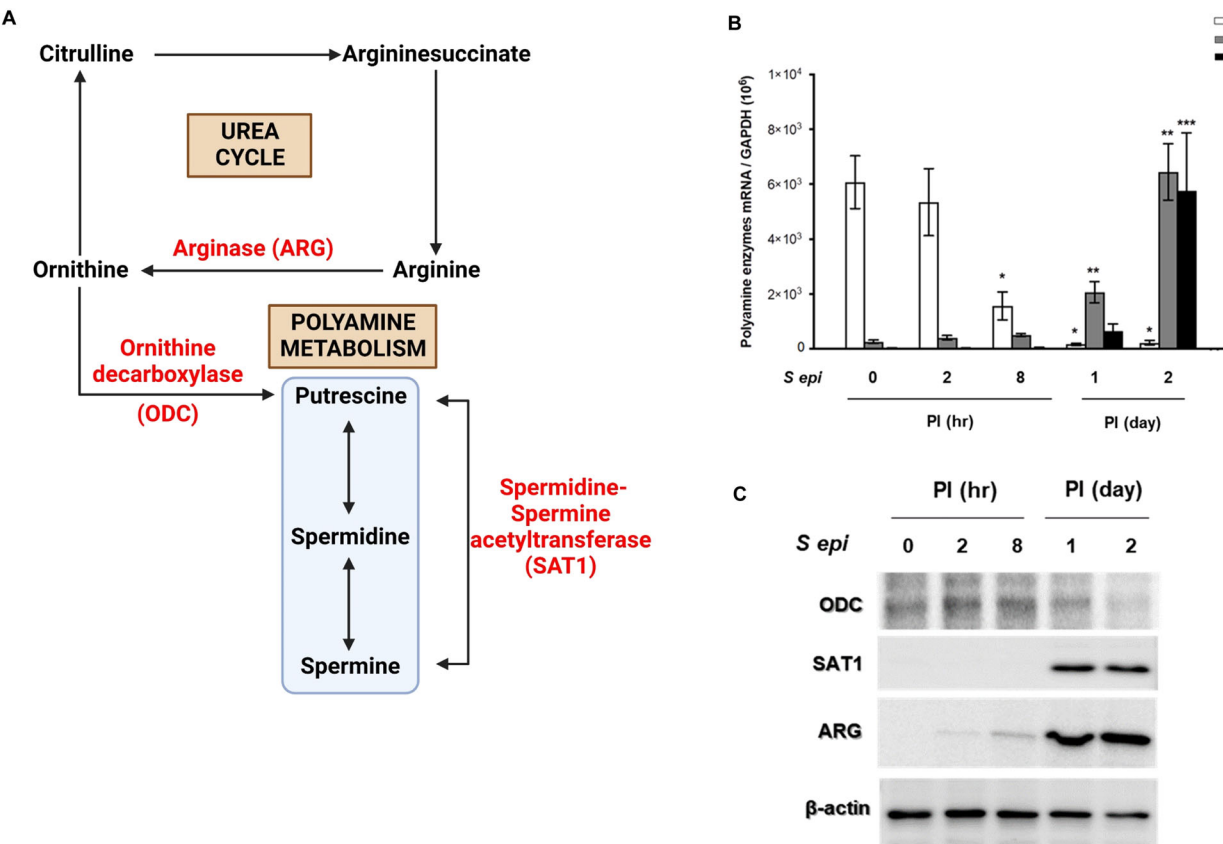


Fig. 4 | *Staphylococcus epidermidis* creates a polyamine-depleted cellular environment by affecting enzymes involved in polyamine production. *Staphylococcus epidermidis* creates a polyamine-depleted cellular environment by affecting enzymes

involved in polyamine production. A Schematic diagram of the urea cycle and polyamine metabolism, and B mRNA levels of polyamine enzymes and C protein expression of each enzyme.

limited in the nasal epithelium after the inoculation of *S. epidermidis*. We postulated that *S. epidermidis* might help to disrupt the spread of IAV from the upper airway to the respiratory tract and mediates a distinctive antiviral host–bacterial commensalism in the nasal epithelium.

Polyamines are found in all mammalian cells, although at various concentrations in different organisms and within the context of a normal healthy cell, polyamines are involved in diverse cellular processes including protein synthesis, RNA folding and bending, membrane interactions, protein–RNA interactions, DNA structure, and gene expression^{14,15}. Given the abundance of polyamines within the cell and the importance of these molecules for nucleotide charge neutralization, it is not entirely surprising that viruses manipulate polyamines for their own replication and rely on polyamines for numerous stages in their life cycle. In addition, some viruses also appear to stimulate polyamine synthesis upon infection, highlighting the importance of polyamine production for viral replication¹⁸. Therefore, inhibitors of polyamine biosynthesis may directly inhibit viral translation or may suppress the cellular factors which are essential to the metabolic process of virus replication. Indeed, we showed that IAV replication was significantly reduced in nasal epithelial cells in a polyamine-depleted cellular environment and the presence of polyamines might be necessary for IAV replication in nasal epithelium.

Interestingly, the concentration of ornithine, putrescine, spermine, and spermidine in nasal epithelial cells changed following inoculation with *S. epidermidis*. In particular, the concentration of ornithine was markedly increased in both cell lysate and cell supernatant of nasal epithelium in response to *S. epidermidis* but the concentration of putrescine, spermine, and spermidine was completely reduced in cell lysate in concert with higher concentration in cell supernatant. This result led us to believe that the *S. epidermidis* induces the depletion of intracellular polyamines by inhibiting the transition from ornithine to putrescine or mediates the export of

polyamines from the cells. Although we did not measure the levels of polyamine transporter that could be related to the inhibition of extracellular polyamines transport, we determined that the inoculation of *S. epidermidis* might affect the activity of enzymes that are involved in polyamine biosynthesis. Our data revealed that *S. epidermidis* inhibited the expression of ODC1 and increased ARG and SAT1 expression in nasal epithelium. That is, *S. epidermidis* can activate the enzyme involved in the production of ornithine from arginine among the polyamine biosynthesis-related signal pathway and downregulates the activity of the enzyme involved in the production of putrescine from ornithine in nasal epithelium. Furthermore, this also increases the activation of enzymes that promote the extracellular export of spermine and spermidine. Therefore, in the human nasal commensal, *S. epidermidis* induces a polyamine-depleted cellular environment in the nasal epithelium and the completely low intracellular concentration of polyamines disrupts IAV replication.

Our previous data demonstrated the antiviral effect of *S. epidermidis* against IAV infection in nasal epithelium through type III interferon induction and activation of serine protease inhibitors^{8,12}. The current findings also showed that the polyamine-depleted cellular environment in the presence of *S. epidermidis* might be related to an antiviral defense mechanism resulting in disturbing the transcription and translation of IAV in the nasal epithelium.

Interest in the host defense system activated by *S. epidermidis* and cellular metabolites has increased and recent study revealed that *S. epidermidis* contributed the alteration of lipids such as SM or ceramide (Cer)²⁴. Although these metabolites are key constituents of the skin barrier, the depletion of SM reduced the activity of hemagglutinin and neuraminidase of influenza virus and may be directly associated with restriction of viral spread²⁵. Soudani et al. found that the inhibition of Cer through the downregulation of sphingomyelinase, which is an enzyme that converts SM

to Cer, leads to the suppression of influenza virus infection²⁶. Furthermore, glycine and serine metabolism were emphasized for the inhibition of influenza virus replication and SM can be synthesized from serine and palmitoyl-CoA²⁷. Although we emphasized that *S. epidermidis* may restrict IAV replication via modulating the metabolites of epithelial cell in addition to the induction of polyamine depletion, our metabolomics resulting from *S. epidermidis*-inoculated NHNE cells also showed a reduction of glycine and serine metabolites (Fig. 1D). We presume that decreased concentrations of serine and glycine metabolites also can be involved in limiting IAV replication in nasal epithelium via the control of Cer production. Thus, a further study will be required to determine whether *S. epidermidis* might be involved in the alteration of other metabolites in nasal epithelium.

Some studies have proved the influence of polyamine inhibitors that may modulate virus replication and therefore, the targeting of polyamine depletion may be considered an emerging broad therapeutic approach against multiple respiratory viruses that depend on polyamines for their replication^{14,15}. We also propose that polyamine depletion has a strong impact in reducing IAV replication in nasal epithelium and the symbiotic character of *S. epidermidis*-depleted polyamines benefits the host to potentiate the antiviral immune responses which are connected to the host nasal mucosa-*S. epidermidis* interaction, such as induction of interferon, inhibition of cellular entry that we described previously.

The limitations of our study include details in the clarification of cellular mechanisms how *S. epidermidis* affects the two enzymes that are involved in polyamine biosynthesis or cellular export in NHNE cells. Furthermore, the results about the alteration of metabolites following inoculation of *S. epidermidis* were obtained from in vitro experiments. However, nasal commensal *S. epidermidis* which was applied in the present study, were isolated from the nasal mucus of healthy volunteers and metabolome analysis was conducted using cultured fully differentiated nasal epithelial cells which obtained from healthy human nasal mucosa. The present study focused on verifying the hypothesis that *S. epidermidis* could shape a polyamine-depleted cellular environment in the nasal epithelium and we estimate that the interaction between the host and the symbiotic micro-organism occurring in the actual human nasal mucosa might be mimicked by our experimental models.

Here, we described that the nasal commensal *S. epidermidis* impedes IAV replication in the nasal epithelium through the downregulation of polyamine synthesis and induction of cellular export of polyamines. Our findings provide further understanding that polyamine depletion may be a distinctive antiviral strategy to interfere with IAV replication and indicate an alternative antiviral strategy of nasal commensal in favor of host nasal mucosa.

Material and methods

Ethics statement

Participation in this study was voluntary, with written informed consent obtained from all human subjects before enrollment. The institutional review board (IRB) of the Seoul National University College of Medicine approved the protocol for this study (IRB #C2012248 [943]).

Isolation of *S. epidermidis* from human nasal mucus

Previously, nasal mucus from the middle turbinate of healthy volunteers was collected using sterile 3M Quick swabs (3M Microbiology Products, ST Paul, MN, USA) and a rigid 0-degree endoscope in an operating room⁸. The swabs were inserted into the nasal cavities of the subjects without touching either the nostril or the anterior part of the inferior turbinate, which are lined with stratified squamous epithelium, not respiratory epithelium. The swabs were then gently rotated around the middle turbinate. The swabs with mucus were fixed in a fixative solution and were transported immediately to the laboratory for identification and subsequent microbial analysis. For bacterial colony isolation, the mucus was placed in lysogeny broth (LB) plates. After 2 days of incubation, bacterial colonies were obtained from LB plates and the colony of *S. epidermidis* was identified using GS-FLX 454 Pyrosequencing by 16S rRNA Gene Amplification⁸.

To detect possible contamination, negative controls were prepared and subjected to the same procedures. The first step in the analysis was the extraction of DNA from the bacterial pellet. The bacterial DNA from nasal mucosal swab samples was extracted with a Fast DNA Spin Kit for soil (MP Biomedicals, Solon, OH, USA). The extracted DNA was dissolved in sterile water containing 40 µg/mL RNase A and was quantified with a Nano Quant Infinite M200 spectrophotometer (Tecan, Männedorf, Switzerland) using a ratio of absorbance values at 260 and 280 nm (A₂₆₀/A₂₈₀). We have a total of 50 *S. epidermidis* (*S. epi* 1–50) isolated from 50 healthy volunteers, and we used one *S. epidermidis* (*S. epi* 1) in the present study for in vitro experiments.

Clinical information of healthy volunteers

The frozen-storage *S. epidermidis* (Subject 1) and nasal mucosa (Subject 1–5) from a total of five healthy subjects were used in this study: 3 males (mean body mass index 22.4 kg/m²) and 2 females (mean body mass index 20.3 kg/m²), whose mean age was 35.2 years, and who were referred to the Department of Otorhinolaryngology Seoul National University Hospital (Seoul, Korea) primarily for septal surgery between March and May 2019 (Supplementary Table S1). Intranasal endoscopy, computed tomography of the paranasal sinus, and a skin allergy test were performed before sampling. None of the subjects showed signs of infection, and all showed negative results in the allergy test. Those subjects who had taken any kinds of antibiotics within 2 months; who were pregnant or smokers; who had diseases and medication histories related to asthma; and who had any other chronic diseases such as atherosclerosis, hypertension, arrhythmia, congestive heart failure, diabetes mellitus, osteoporosis, hepatitis, cancer, and autoimmune or neurological diseases were excluded. Participation was voluntary and written informed consent was obtained from all participants and the IRB of the Seoul National University College of Medicine approved the protocol of this study (IRB #C2012248 [943]).

Viruses and reagents

Influenza A virus (IAV WS/33: H1N1, ATCC, Manassas, VA, USA) was used to induce acute viral lung infection. Virus stocks were grown in Madin-Darby canine kidney (MDCK) cells in a virus growth medium according to a standard procedure⁴. Briefly, after 48 h incubation at 37 °C, the supernatants were harvested and spun by centrifugation at 5000 × g for 30 min to remove cellular debris. Virus stocks were titrated on MDCK cells using a tissue culture infectious dose assay and stored at –80 °C.

Cell culture

Normal human nasal epithelial (NHNE) cells were cultured as described previously²⁸. Briefly, passage-2 NHNE cells (1 × 10⁵ cells/culture) were seeded in 0.25 ml of culture medium on Transwell clear culture inserts (24.5 mm, with a 0.45-mm pore size; Costar Co., Cambridge, MA, USA). Cells were cultured in a 1:1 mixture of basal epithelial growth medium and DMEM containing previously described supplements. Cultures were grown while submerged for the first 9 days. The culture medium was changed on Day 1, and every other day thereafter. An air-liquid interface (ALI) was created on Day 9 by removing the apical medium and feeding the cultures from the basal compartment only. The culture medium was changed daily after the initiation of the ALI. Antibiotics such as 1% penicillin and streptomycin were added to all subculture media and culture stages and the antifungal agent fungizone (1 ml/1000 ml media; Life Technologies, Grand Island, NY, USA) was added after filtering the media. All experiments described here used cultured nasal epithelial cells 14 days after the creation of the ALI.

Metabolite profiles obtained from cell lysate and cell supernatant

Cell lysate and supernatant were collected after centrifugation (5 min at 18,341 × g and 2 °C). NHNE cell pellets (3 × 10⁶) were collected and suspended using 75 µl of ice-cold ethanol:0.1 M phosphate buffer (85:15, v:v). The mixture was then subjected to three freeze-thaw cycles using liquid nitrogen and then centrifuged for 5 min at 18,341 × g and 2 °C. Metabolites from the cell lysate and cell supernatant were analyzed using a Biocrates

AbsoluteIDQ p180 kit as described previously²¹. The samples were then analyzed with UPLC-MS/MS system (Waters ACQUITY ultra-performance liquid chromatography coupled with AB SCIEX 5500 QTrap mass spectrometer). The data were normalized by using MetIDQ software. Variables that were not detected at levels above 70% were eliminated, and missing values or values below the limit of detection were imputed by one-fifth of the minimum positive values of their corresponding variables using MetaboAnalyst 5.0²⁹.

Real-time PCR

NHNE cells were infected with WS/33 (H1N1) for 1 day, and total RNA was isolated using TRIzol reagent (Life Technology, Seoul, Korea). Complementary DNA (cDNA) was synthesized from 3 µg of RNA with random hexamer primers (Perkin Elmer Life Sciences, Waltham, MA, USA) and Moloney murine leukemia virus reverse transcriptase (Roche Applied Science, Indianapolis, IN, USA). Amplification was performed using TaqMan Universal PCR Master Mix (PE Biosystems, Foster City, CA, USA) according to the manufacturer's protocol. Briefly, amplification reactions with a total volume of 12 µL contained 2 µL of cDNA (reverse transcription mixture), oligonucleotide primers (final concentration of 800 nM), and TaqMan hybridization probe (200 nM). Real-time PCR probes were labeled at the 5' end with carboxyfluorescein (FAM) and the 3' end with the quencher carboxytetramethylrhodamine (TAMRA). To quantify the cellular viral level and host gene expression, cellular RNA was used to generate cDNA. The IAV level was monitored by performing quantitative PCR of the *PA* gene (segment 3) with forward and reverse primers and a probe (5'-ggccgactacactctcgatga-3', 5'-tgtcttatgttgcataatgcctggtt-3', or 5'-agcaggcttagtc-3'). Primers for human *ODC*, *arginase* (*ARG*), and *spermine or spermidine acetyl transferase 1* (*SAT1*) were purchased from Applied Biosystems (Foster City, CA, USA). Real-time PCR was performed using the PE Biosystems ABI PRISM® 7700 sequence detection system. Thermocycling parameters were as follows: 50 °C for two minutes, 95 °C for 10 min, then 40 cycles of 95 °C for 15 s and 60 °C for one minute. Target mRNA levels were quantified using target-specific primer and probe sets for *PA* gene, *ODC*, *ARG*, and *SAT1*. All reactions were performed in triplicate, and all real-time PCR data were normalized to the level of glyceraldehyde phosphate dehydrogenase (GAPDH, 1 × 10⁶ copies) to correct for variations between samples.

Viral titer determination

Viral titers were determined using a plaque assay. Virus samples were serially diluted with PBS. Confluent monolayers of MDCK cells in 12-well plates were washed twice with PBS, then infected in duplicate with 250 µL/well dilution of each virus. The plates were incubated at 37 °C for 45 min to facilitate virus adsorption. Following adsorption, a 1% agarose overlay in complete MEM supplemented with TPCK trypsin (1 µg/mL) and 1% fetal bovine serum was applied. The plates were then incubated at 37 °C, and cells were fixed with 10% formalin at 2 days post-infection (dpi).

Western blot analysis

The IAV NP, ODC, SAT1, and ARG protein levels were assessed using western blot analysis. IAV NP antibody (molecular weight 55 kDa, primary antibody 1:500) was purchased from Fitzgerald (North Acton, MA, USA, cat #10R-2121). Human ODC1 antibody (molecular weight 61 kDa, cat# MAB2695-SP, primary antibody 1:500), anti-β-actin antibody (molecular weight 43 kDa, primary antibody 1:500), and human SAT1 antibody (molecular weight 20 kDa, cat #AF-1786) were purchased from R&D Systems (Minneapolis, MN, USA). The human ARG antibody (molecular weight 35 kDa, primary antibody 1:500) was purchased from Abcam (Waltham, MA, USA, cat #ab66705). The NHNE cells were lysed with 2× lysis buffer (250 mM Tris-Cl, pH of 6.5, 2% SDS, 4% β-mercaptoethanol, 0.02% bromophenol blue, and 10% glycerol). Cell lysate (30 µg of protein) was electrophoresed in 10% SDS gels and transferred to polyvinylidene difluoride membranes in Tris-buffered saline (TBS; 50 mM Tris-Cl, pH of 7.5, 150 mM of NaCl) for one hour at room temperature. The membrane

was incubated overnight with primary antibody (1:500) in Tween-TBS (TTBS; 0.5% Tween-20 in TBS). After washing with TTBS, the blot was incubated for one hour at room temperature with a secondary anti-rabbit or anti-mouse antibody (1:1,000, Cell Signaling Technologies, Danvers, MA, USA) in TTBS and was visualized using an ECL system (Amersham, Little Chalfont, UK). Raw figures of western blot analysis were shown in Supplementary Fig. S3.

Data analysis

All data are shown as the mean ± standard error of the mean (SEM). Statistical analyses for comparisons were made using the Mann-Whitney U test and Prism8 (GraphPad Software, San Diego, CA, USA). The statistical significance was defined as *p* < 0.05 (*) and *p* < 0.01 (**). Partial least squares-discriminant analysis (PLS-DA) was calculated with MetaboAnalyst 5.0. Metabolite set enrichment analysis (MSEA) using significant metabolites (*p* < 0.05) was analyzed with MetaboAnalyst 5.0 in an SMPDB-based database. Chemical and biochemical relationships of all the detected metabolites were conceived by mapping onto MetaMapp and visualized with Cytoscape 3.8.2^{30,31}.

Reporting summary

Further information on research design is available in the Nature Portfolio Reporting Summary linked to this article.

Data availability

The authors can confirm that all relevant data are included in the manuscript and its supplementary information files. The data about IAV-regulated polyamine metabolism are shown in Supplementary Fig. S1 and DENSpm-induced polyamine depletion in NHNE cells are also shown in Supplementary Fig. S2. The underlying source data about real-time PCR, metabolomics, and raw figures of western blots in Figs. 2, 3, and 4 are presented in a supplementary data set.

Received: 16 August 2023; Accepted: 8 August 2024;

Published online: 22 August 2024

References

1. An, S. et al. Initial Influenza Virus Replication Can Be Limited in Allergic Asthma Through Rapid Induction of Type III Interferons in Respiratory Epithelium. *Front. Immunol.* **9**, 986 (2018).
2. Shin, H. et al. Intranasal inoculation of IFN-λ resolves SARS-CoV-2 lung infection via the rapid reduction of viral burden and improvement of tissue damage. *Front. Immunol.* **13**, 1009424 (2022).
3. Galani, I. E. et al. Interferon-λ Mediates Non-redundant Front-Line Antiviral Protection against Influenza Virus Infection without Compromising Host Fitness. *Immunity* **46**, 875–890 (2017).
4. Kim, S. et al. The Superiority of IFN-λ as a Therapeutic Candidate to Control Acute Influenza Viral Lung Infection. *Am. J. Respir. Cell. Mol. Biol.* **56**, 202–212 (2017).
5. Won, J. et al. Inhaled delivery of Interferon-lambda restricts epithelial-derived Th2 inflammation in allergic asthma. *Cytokine* **119**, 32–36 (2019).
6. Brestoff, J. R. & Artis, D. Commensal bacteria at the interface of host metabolism and the immune system. *Nat. Immunol.* **14**, 676–684 (2013).
7. Liu, Q. et al. *Staphylococcus epidermidis* contributes to healthy maturation of the nasal microbiome by stimulating antimicrobial peptide production. *Cell. Host. Microbe* **27**, 68–78 (2020).
8. Kim, H. J. et al. Nasal commensal *Staphylococcus epidermidis* enhances interferon-λ-dependent immunity against influenza virus. *Microbiome* **7**, 80 (2019).
9. Sahin-Yilmaz, A. & Naclerio, R. M. Anatomy and physiology of the upper airway. *Proc. Am. Thorac. Soc.* **8**, 31–39 (2011).
10. Bassis, C. M. et al. The nasal cavity microbiota of healthy adults. *Microbiome* **2**, 27 (2014).

11. Bassis, C. M. et al. Analysis of the upper respiratory tract microbiotas as the source of the lung and gastric microbiotas in healthy individuals. *MBio* **6**, e00037 (2015).
12. Jo, A. et al. Nasal symbiont *Staphylococcus epidermidis* restricts the cellular entry of influenza virus into the nasal epithelium. *NPJ Biofilms Microbiomes* **8**, 26 (2022).
13. Laporte, M. & Naesens, L. Airway proteases: an emerging drug target for influenza and other respiratory virus infections. *Curr. Opin. Virol.* **24**, 16–24 (2017).
14. Firpo, M. R. et al. Targeting Polyamines Inhibits Coronavirus Infection by Reducing Cellular Attachment and Entry. *Acs. Infect. Dis.* **7**, 1423–1432 (2021).
15. Huang, M. et al. Targeting Polyamine Metabolism for Control of Human Viral Diseases. *Infect. Drug. Resist.* **13**, 4335–4346 (2020).
16. Mounce, B. C. et al. Polyamines and Their Role in Virus Infection. *Microbiol. Mol. Biol. Rev.* **81**, e00029–17 (2017).
17. Mounce, B. C. et al. Interferon-Induced Spermidine-Spermine Acetyltransferase and Polyamine Depletion Restrict Zika and Chikungunya Viruses. *Cell. Host. Microbe* **20**, 167–177 (2016).
18. Tate, P. M., Mastrodomenico, V. & Mounce, B. C. Ribavirin Induces Polyamine Depletion via Nucleotide Depletion to Limit Virus Replication. *Cell. Rep.* **28**, 2620–2633 (2019).
19. Oredsson, S. M. et al. Inhibition of cell proliferation and induction of apoptosis by N(1),N(11)-diethylhorspermine-induced polyamine pool reduction. *Biochem. Soc. Trans.* **35**, 405–409 (2007).
20. Pegg, A. E. The role of polyamine depletion and accumulation of decarboxylated S-adenosylmethionine in the inhibition of growth of SV-3T3 cells treated with alpha-difluoromethylornithine. *Biochem. J.* **224**, 29–38 (1984).
21. Iwasaki, A. & Pillai, P. S. Innate immunity to influenza virus infection. *Nat. Rev. Immunol.* **14**, 315–328 (2014).
22. Pang, I. K. & Iwasaki, A. Inflammasomes as mediators of immunity against influenza virus. *Trends Immunol.* **32**, 34–41 (2011).
23. Segal, L. N., Rom, W. N. & Weiden, M. D. Lung microbiome for clinicians. New discoveries about bugs in healthy and diseased lungs. *Ann. Am. Thorac. Soc.* **11**, 108–116 (2014).
24. Zheng, Y. et al. Commensal *Staphylococcus epidermidis* contributes to skin barrier homeostasis by generating protective ceramides. *Cell. Host. Microbe* **30**, 301–313 (2022).
25. Tafesse, F. G. et al. Intact sphingomyelin biosynthetic pathway is essential for intracellular transport of influenza virus glycoproteins. *Proc. Natl Acad. Sci. USA* **110**, 6406–6411 (2013).
26. Soudani, N. et al. Ceramide Suppresses Influenza A Virus Replication In Vitro. *J. Virol.* **93**, e00053–19 (2019).
27. Hanada, K. Serine palmitoyltransferase, a key enzyme of sphingolipid metabolism. *Biochim. Biophys. Acta* **1632**, 16–30 (2003).
28. Ji, J. Y. et al. The nasal symbiont *Staphylococcus* species restricts the transcription of SARS-CoV-2 entry factors in human nasal epithelium. *iScience* **24**, 103172 (2021).
29. Pang, Z. et al. Using MetaboAnalyst 5.0 for LC-HRMS spectra processing, multi-omics integration and covariate adjustment of global metabolomics data. *Nat. Protoc.* **17**, 1735–1761 (2022).
30. Barupal, D. K. et al. MetaMapp: mapping and visualizing metabolomic data by integrating information from biochemical pathways and chemical and mass spectral similarity. *Bmc. Bioinforma.* **13**, 99 (2012).
31. Polyzos, A. A. et al. Metabolic Reprogramming in Astrocytes Distinguishes Region-Specific Neuronal Susceptibility in Huntington Mice. *Cell. Metab.* **29**, 1258–1273 (2019).

Acknowledgements

This work was supported by the Basic Science Research Program through the National Research Foundation of Korea, funded by the Ministry of Education (2022R1A2C2011867) awarded to H.J.K. and by the Ministry of Science and ICT (RS 2023-00222762), Korea awarded to H.J.K. This research was also supported by a grant from the Korean Health Technology R&D Project through the Korean Health Industry Development Institute, funded by the Ministry of Health and Welfare of the Republic of Korea (HI23C0795 awarded to H.J.K.). This work was supported by the National Research Foundation of Korea (NRF) grant funded by the Korea government (MSIT) (NRF-2022R1A2C2005651) awarded J.Y.C.

Author contributions

H.J.K., and J-Y.C. conceived the study and designed the experiments. A.J., K-S.K., and H.J.K. carried out the study, including sample collection and sample preparation. K-S.K., J.W., H.S. and S.K. performed additional work, design, and data analysis. B.K., and D.J.K. carried out additional data analysis. H.J.K., and J-Y.C. drafted the manuscript.

Competing interests

The authors declare no competing interests.

Additional information

Supplementary information The online version contains supplementary material available at <https://doi.org/10.1038/s42003-024-06706-4>.

Correspondence and requests for materials should be addressed to Joo-Youn Cho or Hyun Jik Kim.

Peer review information *Communications Biology* thanks the anonymous reviewers for their contribution to the peer review of this work. Primary Handling Editors: Shitao Li and Tobias Goris. A peer review file is available.

Reprints and permissions information is available at <http://www.nature.com/reprints>

Publisher's note Springer Nature remains neutral with regard to jurisdictional claims in published maps and institutional affiliations.

Open Access This article is licensed under a Creative Commons Attribution-NonCommercial-NoDerivatives 4.0 International License, which permits any non-commercial use, sharing, distribution and reproduction in any medium or format, as long as you give appropriate credit to the original author(s) and the source, provide a link to the Creative Commons licence, and indicate if you modified the licensed material. You do not have permission under this licence to share adapted material derived from this article or parts of it. The images or other third party material in this article are included in the article's Creative Commons licence, unless indicated otherwise in a credit line to the material. If material is not included in the article's Creative Commons licence and your intended use is not permitted by statutory regulation or exceeds the permitted use, you will need to obtain permission directly from the copyright holder. To view a copy of this licence, visit <http://creativecommons.org/licenses/by-nc-nd/4.0/>.

© The Author(s) 2024